Hindawi
Shock and Vibration
Volume 2022, Article ID 3238461, 10 pages
https://doi.org/10.1155/2022/3238461

Research Article

Feature Extraction of Ship-Radiated Noise Based on Hierarchical Dispersion Entropy

Leilei Xiao

Xi'an Traffic Engineering Institute, Xi'an, Shaanxi 710300, China

Correspondence should be addressed to Leilei Xiao; dierxiaoleilei1982@163.com

Received 9 April 2022; Revised 30 April 2022; Accepted 13 May 2022; Published 28 May 2022

Academic Editor: Yuxing Li

The classification and recognition of ship-radiated noise (SRN) is of great significance to the processing of underwater acoustic signals. In order to improve the stability of recognition and more accurately identify SRN, single feature extraction and dual feature extraction based on hierarchical dispersion entropy (HDE) are proposed. For single feature extraction, HDE of the best node among the eight nodes of the third layer decomposition is extracted. For dual feature extraction, HDE of the best two nodes among the 14 nodes of the first-, second-, and third-layer decompositions are required. The results show that the recognition rate of single and dual feature extraction originated from the method based on HDE reaches 85% and 100%, respectively, better than the method of hierarchical reverse dispersion entropy (HRDE) and hierarchical permutation entropy (HPE).

1. Introduction

SRN is the signal generated by engine vibration during ship navigation, which contains a lot of feature information about the ship underway [1–3]. The commonly used features are time-domain features [4], frequency-domain features [5], and auditory features [6]. However, affected by the complex marine environment, the collected SRN signals often have the characteristics of nonlinearity and nonstationary, and the traditional features cannot guarantee the separability and stability [7–12]. Therefore, it is very important to find a feature suitable for characterizing the SRN.

In recent years, the characteristics of nonlinear dynamics have attracted many scholars' attention because of their advantages in representing nonlinear signals. The commonly used nonlinear dynamics features include Lyapunov index [13], fractal dimension [14], Lempel-Ziv complexity [15, 16] and entropy algorithm [17], among which entropy algorithm can be used to represent the amount of information in a period of time, and has been widely used in many fields due to its simplicity of calculation [18, 19]. In 2002, Bandt and Pompe first proposed permutation entropy (PE) and applied it to the detection of biomedical signals [20]. Later, Li et al. improved PE and applied it to the feature extraction of SRN signals, and achieved good results in classification [8]. In 2016, Rostaghi and Azami proposed dispersion entropy (DE) to solve the defect that PE did not take into account the relationship between the amplitudes of time series [21]. Later, Jiao et al. proposed Fluctuation-based reverse dispersion entropy (FRDE) on the basis of DE, which was used in ship signal classification and achieved high recognition rate [22]. In 2019, Cuesta Frau proposed slope entropy (SlEn) based on relative frequency of simple symbol patterns [23], after that, Li combined SlEn with PE to improve the classification and recognition rate of ship signals through the double feature extraction method [24]. In conclusion, it is of great significance to further extract the features of SRN signals based on entropy.

Although these aforementioned entropies have achieved good results in feature extraction of SRN, they all ignore the hierarchical information between signals. HDE can obtain the hierarchical information of signals obtained in the full frequency band. Xue et al. applied HDE to the field of rolling bearing fault diagnosis [25], Ke et al. applied HDE to the weak fault diagnosis scheme of common rail injectors [26], and Song et al. also applied HDE to the fault diagnosis of high pressure common rail injectors [27], and all these paper have achieved good results. Influenced by that, HDE is

applied to SRN recognition in this paper, which fills the gap of HDE application in underwater acoustic field.

In this paper, HDE is introduced into the field of underwater acoustics to identify and classify SRN, hierarchical decomposition of SRN is carried out, and DE features are extracted from the obtained nodes. Section 2 introduces HDE, including hierarchical decomposition and DE. Section 3 represents the proposed method. Section 4 illustrates feature extraction of SRN. Section 5 shows some conclusions obtained from the experiment.

2. Methodology

2.1. Hierarchical Decomposition

(1) For a time series $\{u(i), i = 1, 2, \ldots, N\}$, define the two operators Q_0 and Q_1, as

$$\begin{aligned} Q_0(u) &= \frac{u(2j) + u(2j+1)}{2}, \quad j = 1, 2, \ldots, 2^{n-1}, \\ Q_1(u) &= \frac{u(2j) - u(2j+1)}{2}, \quad j = 1, 2, \ldots, 2^{n-1}, \end{aligned} \tag{1}$$

where $Q_0(u)$ and $Q_1(u)$ represent the low and high-frequency components of signal decomposition; for $j = 0, 1$ the matrix form of Q_j can be shown as

$$Q_j = \begin{pmatrix} \frac{1}{2}\left(-\frac{1}{2}\right)^j & 0 & 0 & \cdots & 0 & 0 \\ 0 & 0 & \frac{1}{2}\left(-\frac{1}{2}\right)^j & \cdots & 0 & 0 \\ 0 & 0 & 0 & 0 & \cdots & \frac{1}{2}\left(-\frac{1}{2}\right)^j \end{pmatrix}_{2^{n-1} \times 2^n}. \tag{2}$$

(2) Construct an n-dimensional vector $[\gamma_1, \gamma_2, \ldots, \gamma_n] \in \{0, 1\}$, the integer e can be expressed as

$$e = \sum_{j=1}^{n} \gamma_j 2^{n-j}. \tag{3}$$

(3) According to vector $[\gamma_1, \gamma_2 \ldots, \gamma_n]$, the decomposition nodes of each layer of the signal are

$$u_{k,e} = Q_{\gamma_n} \cdot Q_{\gamma_{n-1}} \cdot \cdots Q_{\gamma_1}(u). \tag{4}$$

2.2. Hierarchical Dispersion Entropy. DE is an index to measure the irregularity of time series. A larger value of this indicates a higher irregularity of this time series. On the contrary, a smaller value means a smaller irregularity.

For a time series $\{x(i), i = 1, 2, \ldots, N\}$, the DE was calculated as follows:

(1) Mapping time series $x(i)$ to $\{x(j), j = 1, 2, \ldots, N\}$ through a normal distribution function, $y(j) \in (0, 1)$

$$y(j) = \frac{1}{\sigma\sqrt{2\pi}} \int_{-\infty}^{x(i)} e^{\left(-(t-\mu)^2/2\sigma^2\right)} \mathrm{d}t, \tag{5}$$

where μ and σ represent the expectation and variance of x, respectively.

(2) Mapping $y(j)$ to an integer between 1 and c by the following formula:

$$z_j^c = \mathrm{Round}(c \cdot y(j) + 0.5), \tag{6}$$

where Round is an integer function and c is the number of mapped categories.

(3) Calculating embedded vector $z_i^{m,c}$,

$$z_i^{m,c} = \left\{z_i^c, z_{i+d}^c, \ldots, z_{i+(m-1)d}^c\right\}, \tag{7}$$

where m is the embedded dimension and d is the time delay constant.

(4) Calculating the dispersion pattern $\pi_{v_0 v_1 \ldots v_{m-1}}$ $(v = 1, 2, \ldots c)$ for each time series $z_i^{m,c}$, the number of dispersion patterns are c^m, $z_i^c = v_0, z_{i+d}^c = v_1, \cdots z_{i+(m-1)d}^c = v_{m-1}$.

(5) For these patterns, the probability $p(\pi_{v_0 v_1 \ldots v_{m-1}})$ of each dispersion pattern $\pi_{v_0 v_1 \ldots v_{m-1}}$ is

$$p\left(\pi_{v_0 v_1 \ldots v_{m-1}}\right) = \frac{\mathrm{Number}\left(\pi_{v_0 v_1 \ldots v_{m-1}}\right)}{N - (m-1)d}, \tag{8}$$

where $\mathrm{Number}(\pi_{v_0 v_1 \ldots v_{m-1}})$ is the number of dispersion patterns.

(6) DE of time series is defined as

$$DE(x, m, c, d) = -\sum_{\pi=1}^{c^m} p\left(\pi_{v_0 v_1 \ldots v_{m-1}}\right) \ln\left(p\left(\pi_{v_0 v_1 \ldots v_{m-1}}\right)\right). \tag{9}$$

For each node obtained by hierarchical decomposition, its DE is calculated, and all the results obtained are HDE.

3. Proposed Method

This paper recognizes SRN by extracting HDE feature of the signal, and two feature extraction methods, single feature extraction and dual feature extraction are used. The method of identifying SRN using HDE features is shown in Figure 1. The specific steps for single feature extraction are as follows:

(1) Input SRN as the signal to be identified.

(2) Hierarchical decomposition of the signal at the third level, the signal is decomposed into eight nodes.

(3) Selecting the optimal node and calculating its DE as the feature of SRN.

(4) Classify and recognize the obtained features by k-nearest neighbor (KNN) to get the recognition result of the signal.

Dual feature extraction and single feature extraction are the same except for the second and third steps; in the second

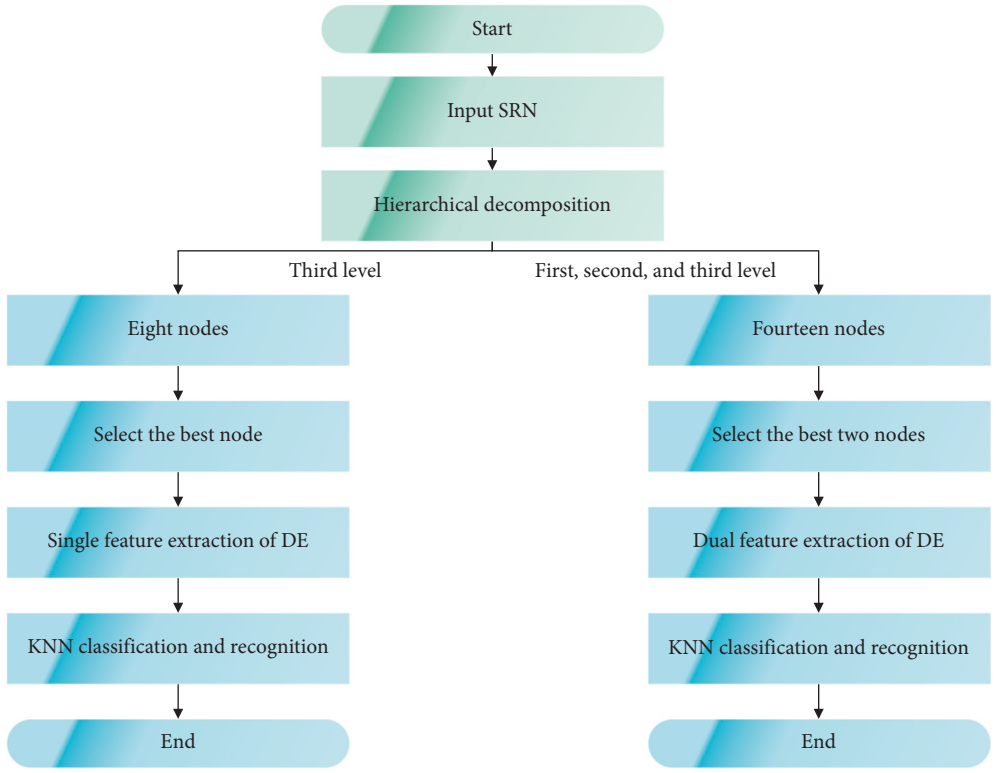

Figure 1: The method of identifying SRN using HDE features.

step, dual feature extraction requires fourteen nodes derived from the first-, second-, and third-level decomposition of the signal; in the third step, two optimal nodes are selected.

4. Feature Extraction of Ship-Radiated Noise

4.1. Ship-Radiated Noise. Feature extraction and classification recognition of four types of SRN are carried out. These four types of signals are identified as SRN1, SRN2, SRN3, and SRN4. The signal lengths of the first and second types are 1380000, the third type are 2828835, and the fourth type are 1641600, and the sampling frequency is 44.1 kHz. Take data points from 1 to 1200000 of the four types of SRN. Figure 2 presents four types of SRN after normalization.

4.2. Feature Extraction Experiment

4.2.1. Single Feature Extraction. In this section, we extract the features of four types of SRN. First, hierarchical decomposition of SRN is carried out, then take eight nodes of the third-level decomposition and extract their DE features. This is called HDE of the third-level decomposition of SRN. Then, as a comparison, we extract the reverse dispersion entropy and PE of the nodes separately, these are called HRDE and HPE of the third-level decomposition, respectively.

The HDE of eight nodes for four types of SRN is extracted, and the sample distribution is observed. The HDE of eight nodes for four types of SRN is shown in Figure 3.

It can be seen from the diagram that the HDE of the four types of SRN in the Node 1 is quite different. There are duplicate parts of the HDE of SRN1 and SRN4, and the same is true of SRN2 and SRN3; there is no significant difference in HDE between the four types of SRN in Node 2 to Node 7; HDE of SRN2 in Node 8 differs significantly from the other three types. The HRDE of eight nodes for four types of SRN can be seen in Figure 4.

The results of feature extraction show that there is no obvious difference among the four types of SRN samples under the same node; the difference of HRDE is obvious only under Node1; of the remaining seven nodes, a few samples of SRN 3 had significant differences in HRDE; in Node 2, HRDE of SRN1 is somewhat different from the other three types of SRN. Figure 5 displays the HPE of eight nodes for four types of SRN.

It can be seen from the figure that there are many differences in HPE for the four types of SRN only in the first node, but the range of entropy values for each type of SRN sample still has a large repetition; the sample entropy values of SRN2 and other SRN in the eighth node are different; the entropy values of four types of SRN from Node 2 to Node 7 differ little except for a small number of samples; differences of HPE between the four types of SRN are small, making it difficult to distinguish them effectively.

4.2.2. Results of Classification. Using k-nearest neighbor to recognize the results of feature extraction, the value of K was 1. Fifty training samples are used for each type of SRN, and the rest are used as test samples to classify and identify the four types of SRN. The validity of the feature extraction method proposed in this paper is verified by comparing the

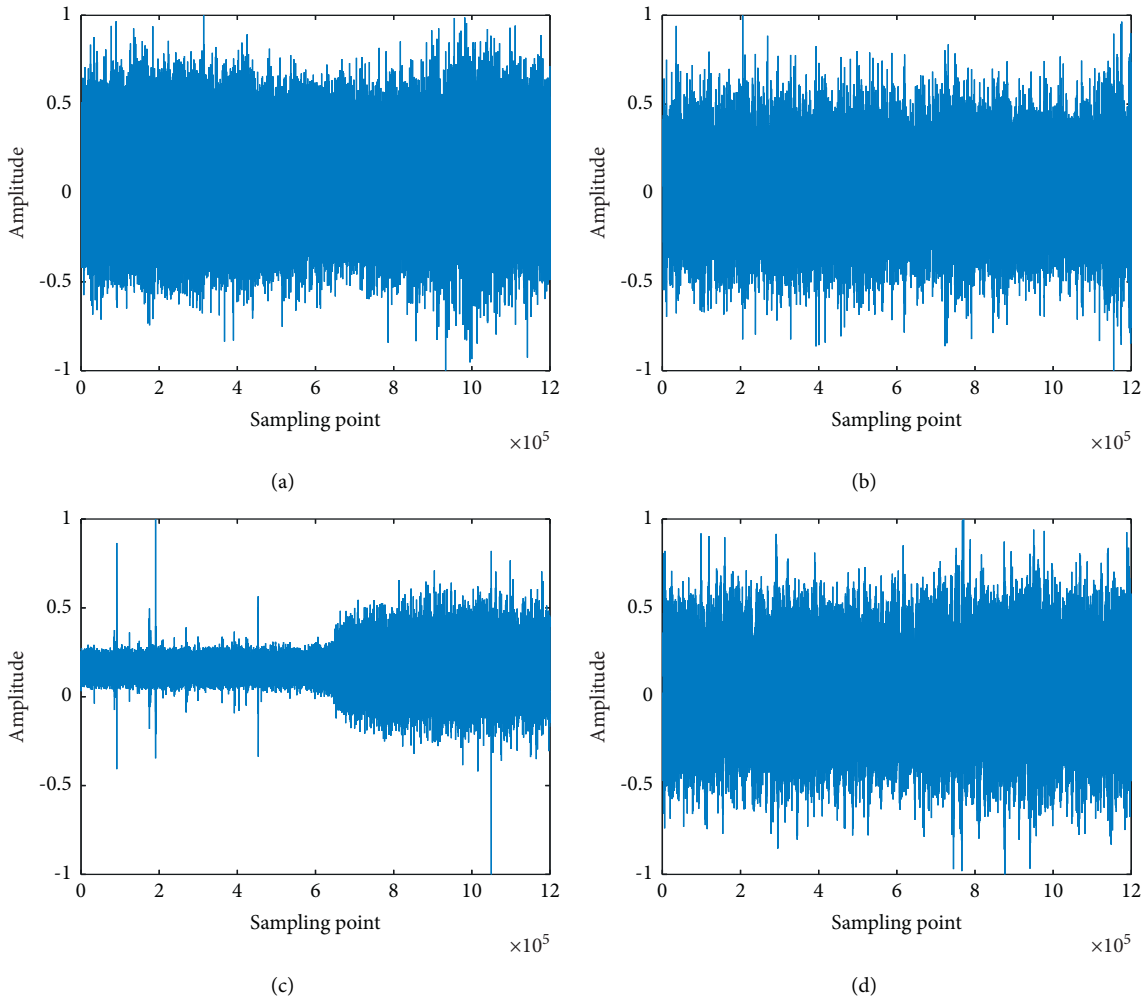

Figure 2: Four types of SRN after normalization. (a) SRN1. (b) SRN2. (c) SRN3. (d) SRN4.

recognition rates of the four feature extraction methods. The HDE recognition rate for four types of SRN is shown in Table 1.

It can be seen from Table 1 that the recognition results of four types of SRN are not good, and the highest average recognition rate is 85%; the highest recognition rate is 96% of the eight nodes for four types of SRN, and the lowest recognition rate is only 16%. The recognition rate of each node of SRN3 and SRN4 is less than 90%. Node 4 and Node 7 have recognition rates of less than 50%, and the HRDE recognition rates for four types of SRN are presented in Table 2.

As can be seen from Table 2, the HRDE of the eight nodes for four types of SRN has the highest recognition rate of 100% and the lowest recognition rate of 22%; the average recognition rate of Node 1 is 82.5%, but the average recognition rate of the remaining seven nodes is not more than 50%; the highest recognition rate of SRN2 appeared in Node 8, and the highest recognition rate of the other three types of SRN appeared in Node 1; the identification rate of all nodes in SRN3 is lower than 80%. In general, the recognition results are not good for distinguishing the four types of SRN. Table 3 shows the HPE recognition rate for four types of SRN.

According to Table 3, the results of HPE recognition of eight nodes for four types of SRN are poor, with the highest average recognition rate is only 60.5%; the recognition rate of the four types of SRN from Node 2 to Node 7 is less than 60%; in SRN2, the recognition rate of Node 1 and Node 8 is significantly higher than that of other nodes; besides SRN2, the highest recognition rate of all nodes of the three types of SRN is only 54%; it is difficult to distinguish four kinds of SRN by HPE.

Because the recognition results obtained by single feature extraction for eight nodes after three-level decomposition are not obvious, which is difficult to distinguish four types of SRN, consider adding more nodes and improving the feature extraction method. Dual feature extraction experiments are performed on fourteen nodes of the first-, second-, and third-level decomposition results.

4.3. Dual Feature Extraction Experiment. The results of hierarchical decomposition consist of fourteen nodes, third-level decomposition as the first to eight nodes, second-level decomposition as the ninth to twelfth nodes, and first-level decomposition as the thirteenth and fourteenth nodes.

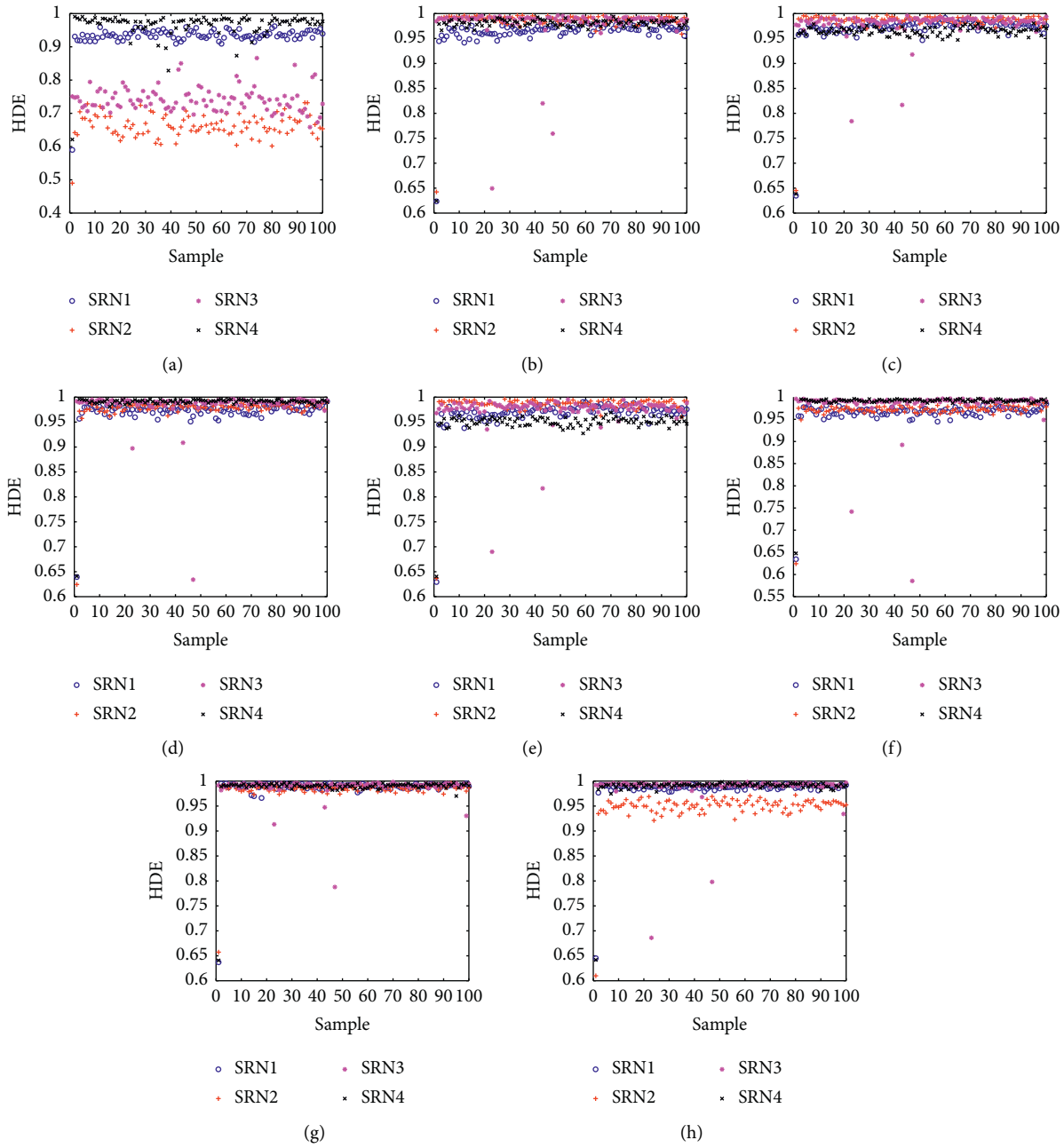

Figure 3: HDE of eight nodes for four types of SRN. (a) Node 1. (b) Node 2. (c) Node 3. (d) Node 4. (e) Node 5. (f) Node 6. (g) Node 7. (h) Node 8.

Feature distribution and recognition rate of the optimal result of dual feature recognition of four types of SRN are shown in Figure 6 and Table 4.

From Figure 6, we can see that the dual feature distribution of the same feature of the four types of SRN is significantly different, and the general distribution range of the four types of SRN can be clearly identified besides a very small number of samples.

It can be seen from Table 4 that in the dual feature extraction experiment, the recognition effect of the HDE is the best, and the highest recognition rate reaches 100%; among the three, the HPE has the worst recognition effect, and the highest recognition rate is 98.5%; the combination with the highest HDE recognition rate is Node 6 and Node 13, and the combination with the highest HRDE and HPE recognition rate is Node 1 and Node 13.

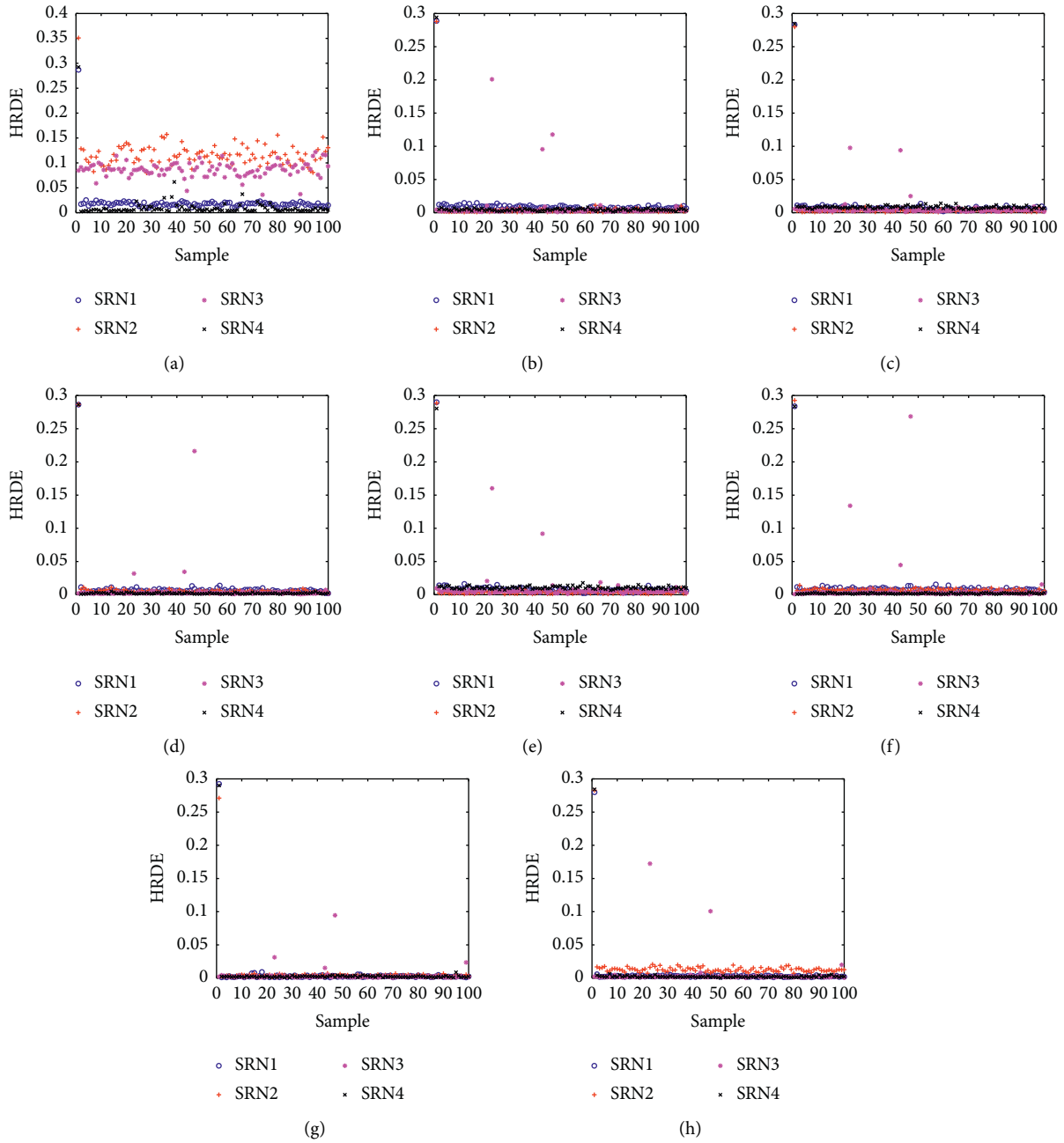

Figure 4: HRDE of eight nodes for four types of SRN. (a) Node 1. (b) Node 2. (c) Node 3. (d) Node 4. (e) Node 5. (f) Node 6. (g) Node 7. (h) Node 8.

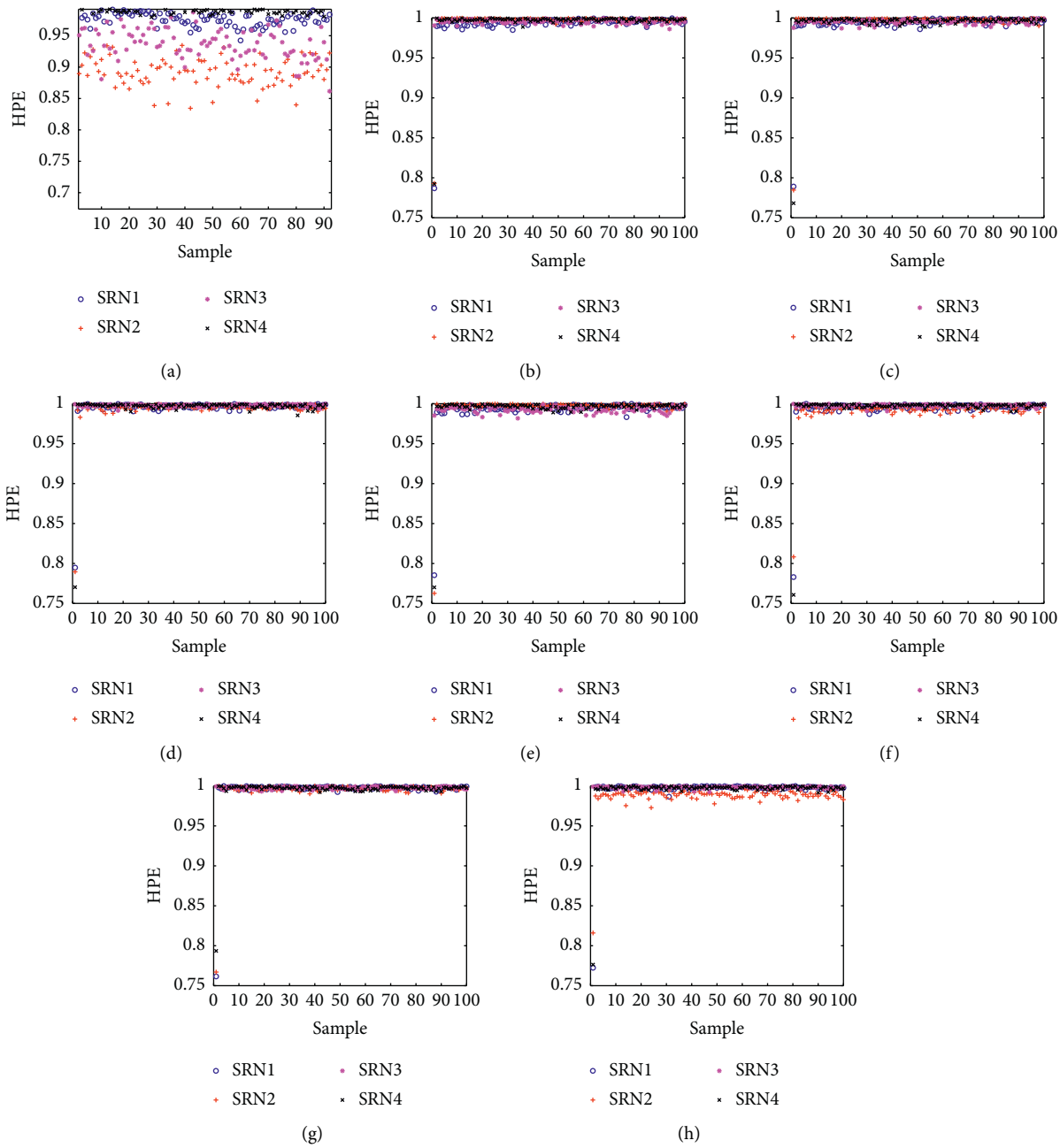

Figure 5: HPE of eight nodes for four types of SRN. (a) Node 1. (b) Node 2. (c) Node 3. (d) Node 4. (e) Node 5. (f) Node 6. (g) Node 7. (h) Node 8.

Table 1: HDE recognition rates for four types of SRN.

	SRN1 (%)	SRN2 (%)	SRN3 (%)	SRN4 (%)	Average (%)
Node 1	92	86	76	86	85
Node 2	56	42	16	52	41.5
Node 3	40	64	38	42	46
Node 4	44	36	40	38	39.5
Node 5	50	72	50	64	59
Node 6	58	34	56	52	50
Node 7	24	42	28	22	29
Node 8	48	96	38	34	54

Table 2: HRDE recognition rates for four types of SRN.

	SRN1 (%)	SRN2 (%)	SRN3 (%)	SRN4 (%)	Average (%)
Node 1	92	78	74	86	82.5
Node 2	42	40	30	46	39.5
Node 3	42	64	40	54	50
Node 4	48	26	38	56	42
Node 5	24	56	40	58	44.5
Node 6	48	48	48	56	50
Node 7	36	40	22	28	31.5
Node 8	40	100	26	32	49.5

Table 3: HPE recognition rates for four types of SRN.

	SRN1 (%)	SRN2 (%)	SRN3 (%)	SRN4 (%)	Average (%)
Node 1	54	82	54	52	60.5
Node 2	26	20	52	26	31
Node 3	26	36	18	22	25.5
Node 4	20	34	36	36	31.5
Node 5	24	56	38	22	35
Node 6	28	40	48	30	36.5
Node 7	36	24	20	24	26
Node 8	34	80	32	36	45.5

Table 4: Recognition rate of the optimal result of dual feature recognition for four types of SRN.

	HDE	HRDE	HPE
Recognition rate	100%	99%	98.5%
Node	6, 13	1, 13	1, 13

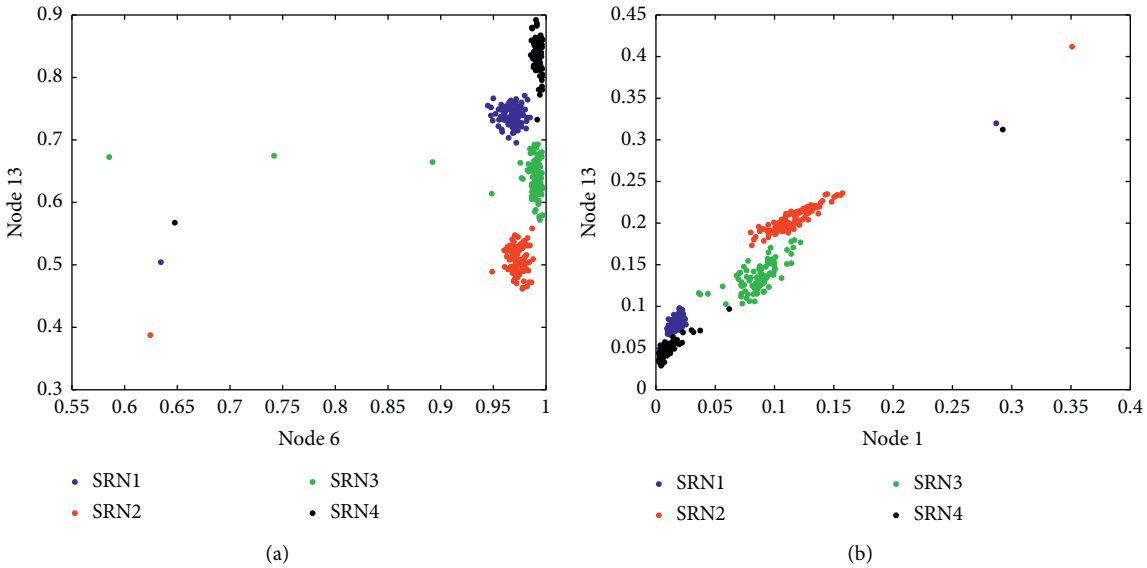

(a) (b)

Figure 6: Continued.

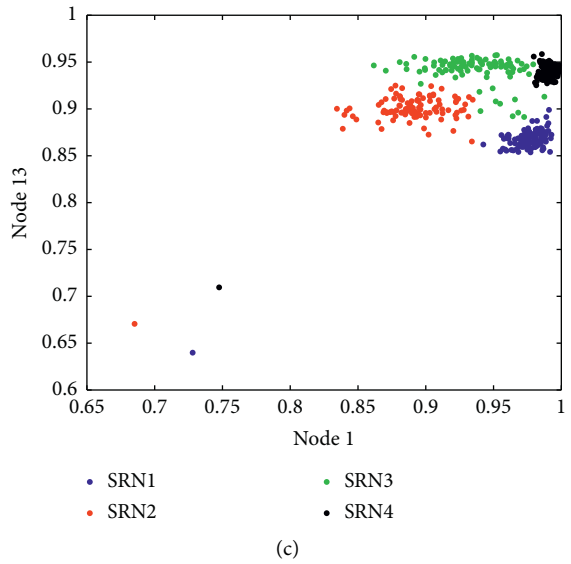

(c)

Figure 6: Feature distribution of the optimal result of dual feature recognition for four types of SRN. (a) HDE. (b) HRDE. (c) HPE.

5. Conclusions

In this paper, HDE is introduced into the feature extraction field of SRN, and single feature extraction and double feature extraction methods based on HDE are proposed. The final recognition rate reaches 100%, which verifies the effectiveness of HDE, and the main conclusions of the experiments are as follows:

(1) HDE can show the high-frequency and low-frequency feature of signals, and it is often used in fault diagnosis of rolling bearings. This paper introduces it into the field of SRN recognition as a new feature of SRN.

(2) Compared with the extractions of HRDE and HPE, the recognition result of HDE single feature recognition can better distinguish SRN.

(3) In order to further improve the performance of HDE in feature extraction, a dual feature extraction method is proposed. The recognition rate is significantly improved compared with the single feature, and the recognition effect is better than the dual feature recognition of the other two feature extraction methods.

Data Availability

The data that support the findings of this study are available on request from the corresponding author.

Conflicts of Interest

The authors declare that they have no conflicts of interest.

References

[1] S. Wang and X. Zeng, "Robust underwater noise targets classification using auditory inspired time frequency analysis," *Applied Acoustics*, vol. 78, no. 4, pp. 68–76, 2014.

[2] F. Yuan, X. Ke, and E. Cheng, "Joint representation and recognition for ship-radiated noise based on multimodal deep learning," *Journal of Marine Science and Engineering*, vol. 7, no. 11, p. 380, 2019.

[3] S. Shen, H. Yang, and M. Sheng, "Compression of a deep competitive network based on mutual information for underwater acoustic targets recognition," *Entropy*, vol. 20, no. 4, p. 243, 2018.

[4] W. Zhao, J. Yang, Z. Hu, and L. Tao, "Coupled analysis of nonlinear sloshing and ship motions," *Applied Ocean Research*, vol. 47, pp. 85–97, 2014.

[5] A. Banazadeh, M. S. Seif, M. J. Khodaei, and M. Rezaie, "Identification of the equivalent linear dynamics and controller design for an unmanned underwater vehicle," *Ocean Engineering*, vol. 139, pp. 152–168, 2017.

[6] J. Li and H. Yang, "The underwater acoustic target timbre perception and recognition based on the auditory inspired deep convolutional neural network," *Applied Acoustics*, vol. 182, Article ID 108210, 2021.

[7] Y. Li, X. Chen, and J. Yu, "A hybrid energy feature extraction approach for ship-radiated noise based on CEEMDAN combined with energy difference and energy entropy," *Processes*, vol. 7, no. 2, p. 69, 2019.

[8] Y.-X. Li, Y.-A. Li, Z. Chen, and X. Chen, "Feature extraction of ship-radiated noise based on permutation entropy of the intrinsic mode function with the highest energy," *Entropy*, vol. 18, no. 11, p. 393, 2016.

[9] D. Xie, H. Esmaiel, H. Sun, J. Qi, and Z. A. H. Qasem, "Feature extraction of ship-radiated noise based on enhanced variational mode decomposition, normalized correlation coefficient and permutation entropy," *Entropy*, vol. 22, no. 4, p. 468, 2020.

[10] Y. Li, Y. Li, X. Chen, and J. Yu, "Denoising and feature extraction algorithms using NPE combined with VMD and their applications in ship-radiated noise," *Symmetry*, vol. 9, no. 11, p. 256, 2017.

[11] Y. Li, C. Xiao, and Y. Jing, "The data-driven optimization method and its application in feature extraction of ship-radiated noise with sample entropy," *Energies*, vol. 12, no. 3, p. 356, 2019.

[12] Y. Li, X. Chen, J. Yu, and X. Yang, "A fusion frequency feature extraction method for underwater acoustic signal based on variational mode decomposition, duffing chaotic oscillator

and a kind of permutation entropy," *Electronics*, vol. 8, no. 1, p. 61, 2019.

[13] K. Tee, S. Ge, and E. Tay, "Barrier lyapunov functions for the control of output-constrained nonlinear systems," *IFAC Proceedings Volumes*, vol. 46, no. 20, pp. 449–455, 2013.

[14] R. Lopes and N. Betrouni, "Fractal and multifractal analysis: a review," *Medical Image Analysis*, vol. 13, no. 4, pp. 634–649, 2009.

[15] X. Zhang, R. Roy, and E. Jensen, "EEG complexity as a measure of depth of anesthesia for patients," *IEEE Transactions on Biomedical Engineering*, vol. 48, no. 12, pp. 1424–1433, 2001.

[16] M. Aboy, R. Hornero, D. Abasolo, and D. Alvarez, "Interpretation of the lempel-ziv complexity measure in the context of biomedical signal analysis," *IEEE Transactions on Biomedical Engineering*, vol. 53, no. 11, pp. 2282–2288, 2006.

[17] C. E. Shannon, "A mathematical theory of communication," *Bell System Technical Journal*, vol. 27, no. 4, pp. 623–656, 1948.

[18] S. M. Pincus, "Approximate entropy as a measure of system complexity," *Proceedings of the National Academy of Sciences*, vol. 88, no. 6, pp. 2297–2301, 1991.

[19] Y. Li, X. Gao, and L. Wang, "Reverse dispersion entropy: a new complexity measure for sensor signal," *Sensors*, vol. 19, no. 23, Article ID 5203, 2019.

[20] C. Bandt and B. Pompe, "Permutation entropy: a natural complexity measure for time series," *Physical Review Letters*, vol. 88, no. 17, Article ID 174102, 2002.

[21] M. Rostaghi and H. Azami, "Dispersion entropy: a measure for time-series analysis," *IEEE Signal Processing Letters*, vol. 23, no. 5, pp. 610–614, 2016.

[22] S. Jiao, B. Geng, Y. Li, Q. Zhang, and Q. Wang, "Fluctuation-based reverse dispersion entropy and its applications to signal classification," *Applied Acoustics*, vol. 175, no. 4, Article ID 107857, 2021.

[23] D. Cuesta-Frau, "Slope entropy: a new time series complexity estimator based on both symbolic patterns and amplitude information," *Entropy*, vol. 21, no. 12, p. 1167, 2019.

[24] Y. Li, P. Gao, B. Tang, Y. Yi, and J. Zhang, "Double feature extraction method of ship-radiated noise signal based on slope entropy and permutation entropy," *Entropy*, vol. 24, no. 1, p. 22, 2021.

[25] Q. Xue, B. Xu, C. He et al., "Feature extraction using hierarchical dispersion entropy for rolling bearing fault diagnosis," *IEEE Transactions on Instrumentation and Measurement*, vol. 70, pp. 1–11, 2021.

[26] Y. Ke, C. Yao, and E. Song, "A weak fault diagnosis scheme for common rail injector based on MGOA-MOMEDA and improved hierarchical dispersion entropy," *Measurement Science and Technology*, vol. 32, no. 2, Article ID 025012, 2021.

[27] E. Song, Y. Ke, C. Yao, Q. Dong, and L. Yang, "fault diagnosis method for high-pressure common rail injector based on IFOA-VMD and hierarchical dispersion entropy," *Entropy*, vol. 21, no. 10, p. 923, 2019.